Anal. Chem. 1994, *66*, 963–970

Feasibility of a Chemical Microsensor Based on Surface Plasmon Resonance on Fiber Optics Modified by Multilayer Vapor Deposition

William J. H. Bender* and Raymond E. Dessy
Laboratory Automation and Instrument Design Group, Department of Chemistry, Virginia Polytechnic Institute and State University, Blacksburg, Virginia 24061

Mark S. Miller and Richard O. Claus
Fiber and Electro-Optic Research Center, Bradley Department of Electrical Engineering, Virginia Polytechnic Institute and State University, Blacksburg, Virginia 24061

An intrinsic fiber-optic sensor is described which utilizes the surface plasmon effect to monitor the chemical environment surrounding the fiber. The device is constructed by polishing a short section of the lateral surface of a single-mode fiber to within the evanescent field surrounding the core. Then one or more thin films are deposited onto the polished surface, beginning with a thin metallic film which acts as the support for the plasmon. A highly refractive dielectric overlay is deposited on the metal film to allow the monitoring of a wide range of chemical sample indices of refraction. The final layer applied to the device is the chemical sample of interest. Under the proper conditions the single-mode propagating in the fiber core can be coupled to the surface plasmon mode on the metal film. This coupling is highly dependent on the refractive index of the chemical sample and is seen as a large attenuation of the light reaching the distal terminus of the fiber. A description of the dispersion equation describing sensor operation will be given, along with details on sensor construction and testing.

Recent years have seen increased interest in the areas of chemical sensing and biochemical assay techniques. Surface plasmon resonance is one such technique,[1-3] but SPR has seen little commercial success due to the cumbersome nature of its prism-based experiments. A fiber-optic-based SPR sensor would have a simpler design, would require no laser or detector motion control, would have a simpler sample introduction system, could use disposable sensing elements, and could be microscaled. Existing fiber-based SPR devices are inherently incapable of monitoring aqueous systems whose refractive index range is 1.33–1.35.[4,5] This limitation precludes their use on most practical chemical and biochemical systems. Polishing and thin-film coating of optical fiber surfaces has led to a new SPR sensor device capable of monitoring a wider range of sample refractive indices, including aqueous samples.

THEORY

The phenomenon of surface plasmon resonance (SPR) has been known for several decades. The theory behind the phenomenon is described in a review by Raether.[6] A plasmon is an oscillation of free electrons on the surface of a conductor, typically a metal. The plasmon is excited by the application of an external electric field at the surface of the conductor. The most common method used for generation of surface plasmons is the coupling of transverse-magnetic (TM) polarized energy contained in an evanescent field to the plasmon mode on a metal film. The amount of coupling is extremely sensitive to the refractive indices of the dielectric materials on both sides of the metal film. If one of the dielectric layers consists of a chemical sample, changes in this sample's refractive index can be monitored by measuring changes in the coupling efficiency between the evanescent field and the plasmon.

SPR was first used as a probe to investigate metal surfaces[7,8] and then later as the basis for chemical[9-11] and biochemical[12-14] sensor devices. Initial experiments involved the use of a prism onto which a thin metal film was deposited. The reflection from the prism/metal interface of a p-polarized laser beam was monitored with a photodetector. When the angle of incidence of the laser beam, with respect to the prism/metal interface, was scanned from a highly grazing angle up to near the critical angle (θ_c), a sharp minimum in reflectivity was seen at a very discrete angle. At this angle the wavevector of the laser beam in the prism matched the wavevector of the plasmon, and energy from the laser was coupled to the surface plasmon via the evanescent field at the reflection point. The angular position of the reflectance minimum was strongly

* Address correspondence to this author at The Dow Chemical Company, Louisiana Division Research & Development, P.O. Box 400, Building 2510, Plaquemine, LA 70765.

(1) Gordon, J. G., II; Swalen, J. D. *Opt. Commun.* **1979**, *22*, 374.
(2) Pockrand, I.; Swalen, J. D.; Gordon, J. G., II; Philpott, M. R. *Surf. Sci.* **1977**, *74*, 237.
(3) Lloyd, J. P.; Pearson, C.; Petty, M. C. *Thin Solid Films* **1988**, *160*, 431.
(4) Johnstone, W.; Stewart, G.; Hart, T.; Culshaw, B. *J. Lightwave Technol.* **1990**, *8*, 538.
(5) Zervas, M. *IEEE Photonics Technol. Lett.* **1990**, *12*, 253.
(6) Raether, H. Surface Plasma Oscillations and Their Applications. In *Physics of Thin Solid Films*; Hass, G., Francombe, M., Hoffman, R., Eds.; Academic Press: New York, 1977; Vol. 9, p 145.
(7) Regalado, L. E.; Machorro, R.; Siqueiros, J. M. *Appl. Opt.* **1991**, *30*, 3176.
(8) Robertson, W. M.; Fullerton, E. *J. Opt. Soc. Am.* **1989**, *6*, 1584.
(9) Pockrand, I. *Surf. Sci.* **1978**, *72*, 577.
(10) Nylander, C.; Liedberg, B.; Lind, T. *Sens. Actuators* **1982**, *3*, 79.
(11) Matsubara, K.; Kawata, S.; Minami, S. *Appl. Opt.* **1988**, *27*, 1160.
(12) Liedberg, B.; Nylander, C.; Lundstrom, I. *Sens. Actuators* **1983**, *4*, 299.
(13) Kooyman, R. P. H.; Kolkman, H.; Van Gent, J.; Greve, J. *Anal. Chim. Acta* **1988**, *213*, 35.
(14) Daniels, P. B.; Deacon, J. K.; Eddowes, M. J.; Pedley, D. G. *Sens. Actuators* **1988**, *15*, 11.

0003-2700/94/0366-0963$04.50/0

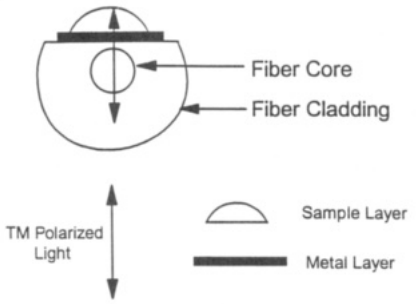

Figure 1. Three-layer sensor geometry.

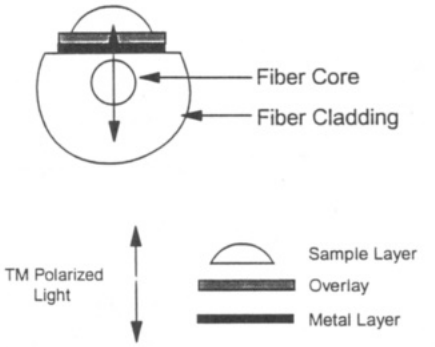

Figure 2. Four-layer sensor geometry.

dependent on the refractive index of any material (sample) coated onto the surface of the metal. An increase in sample refractive index lead to an increase in the angle of minimum reflectivity. Pharmacia Biosensor[15] has produced the only commercially successful prism-based SPR detection system with their BIACore device.

Recent work includes a four-layer chemical sensor that utilizes an extrinsic fiber-optic "light pipe" to deliver optical energy to the prism device,[16] the use of a vibrating mirror to allow rapid scanning of laser launch angles onto the prism/metal interface,[17] and the use of gold-coated diffraction gratings to produce SPR.[18]

If a fiber-optic-based device could be constructed for use as a chemical or biochemical sensor it would have several distinct advantages over the prism-based sensor systems. The fiber device would have no moving parts, would be simpler in design, could use a disposable sensing element, and could be microscaled. SPR has been utilized in the fiber optic communications field as the basis for an in-line, all-fiber polarization device.[4,5] In this configuration a short section of the lateral surface of an optical fiber is polished to within approximately 1 μm of its core, and then a metal film is deposited onto this polished surface. If a crystal or liquid of proper refractive index is placed in contact with the metal film, as shown in Figure 1, TM-polarized radiation in the fiber is coupled to the plasmon wave on the metal film, while TE-polarized energy is allowed to pass. This device has proven to be an effective polarizer but has not been applied to chemical detection.

The dispersion equation given by Johnstone et al.[4] can be solved and plotted for metal thickness as a function of sample refractive index. Thus, for a given target sample refractive index the equation would indicate the proper metal thickness to deposit onto the polished fiber in order to achieve SPR. As we will show later, this system works well as a chemical sensing device but is limited to monitoring samples whose refractive indices are larger than approximately 1.39. This limitation is inherent to optical fibers because of the limited range of cladding refractive indices available. The dispersion equation, which indicates the conditions necessary to achieve the resonance condition, is strongly dependent on cladding index. Most chemical applications for a fiber-based SPR sensor lie in the aqueous index range of 1.33–1.35, so a modification of the fiber sensor is necessary in order to monitor that refractive index range.

If lower refractive index samples are to be monitored, the limitation can been overcome with the application of an overlay material to the metal layer as shown in Figure 2. The plasmon, being a surface effect, is sensitive to only a few hundred nm of material on each side of the metal film. This region will be called the surface plasmon sampling region. The "effective" refractive index of the plasmon sampling region (overlay and chemical sample) is a function of the refractive indices of both the overlay and the sample, and it can be "tuned" to generate the resonance condition for chemical samples of lower refractive index. The "tuning" to various sample refractive indices is controlled by changing either the refractive index of the overlay or its thickness. The higher the refractive index of the overlay, the lower the refractive index of the chemical sample which generates the resonance condition.

The result of the modification is that the four-layer (fiber/metal/overlay/sample) sensor is theoretically capable of monitoring samples whose refractive indices range from 1.00 up to the 1.39 limit inherent in the theree-layer (fiber/metal/sample) sensor. Most importantly, the device is capable of monitoring the 1.33–1.40 aqueous range, where most potential applications are envisioned. The exact sample index which allows surface plasmon resonance is determined by the refractive index and thickness of the overlay.

DERIVATION OF THE DISPERSION EQUATION

In order to predict the behavior of the four-layer sensor, a dispersion equation was derived which relates the optical properties of the layers in the sensor with the generation of surface plasmon resonance. In order to derive the dispersion equation a rigorous analysis of the electric and magnetic fields in all four layers of the sensor must be done. This mathematical treatment is new. It is essential for laying the infrastructure for understanding the need for, and parameters associated with, the various layers that make it possible to construct this family of tunable detectors. The derivation is a very useful tool for others wishing to investigate this type of device. Some readers will be interested in the derivation, others may be interested only in the final results. For the former group the mathematical treatment is included. The latter group may omit reading this section and still gain an understanding of the remainder of the material.

The coordinate system used in deriving the dispersion equation is shown in Figure 3. The layers are stacked along the x axis, and optical propagation is along the z axis. In this work the cladding and sample layers are assumed to be

(15) Pharmacia Biosensor AB, S-751 82 Uppsala, Sweden.
(16) Garces, I.; Aldea, C.; Mateo, J. *Sens. Actuators B* **1992**, *7*, 771.
(17) Lenferink, A. T. M.; Kooyman, R. P. H.; Greve, J. *Sens. Actuators B* **1991**, *3*, 261.
(18) Cullen, D. C.; Brown, R. G. W.; Lowe, C. R. *Biosensors* **1988**, *5*, 211.

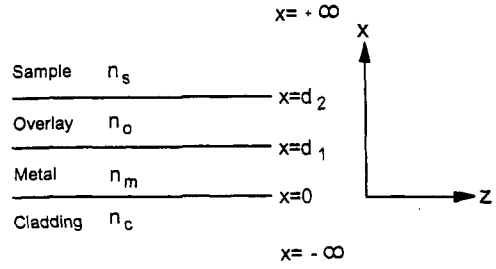

Figure 3. Coordinate system used for solution of dispersion equation.

semiinfinite in thickness as compared to the metal and overlay, and the polished fiber is assumed to approximate a planar waveguide. These assumptions simplify the derivation of the dispersion equation and are supported by Johnstone et al.[4]

The plasmon is a transverse magnetic (TM) effect. This means that only TM, sometimes called P, polarized light in the fiber can be coupled to the plasmon, which transverse electric (TE), sometimes called S, polarized light is unaffected. Therefore, in the derivation of the dispersion equation, only the TM-polarized components, namely the y component of the magnetic field (H_y) and z component of the electric field (E_z), of the light guided by the fiber require consideration. Starting with Maxwell's equations, the one-dimensional waveguide equation for the y component of the magnetic field (H_y) in a TM-polarized electromagnetic wave can be derived as[19]

$$\delta^2 H_y/\delta x^2 + (n^2k^2 - \beta^2)H_y = 0 \qquad (1)$$

where n is the refractive index of the material in which the light is guided, $k = 2\pi/\lambda$, where λ is the optical wavelength, β is the propagation constant of the electromagnetic wave in the material, and the z component of the electric field can be written as

$$E_z = (-i/n^2\omega E_0)\delta H_y/\delta x \qquad (2)$$

where n is the refractive index of the material in which the light is guided, $\omega = 2\pi f$, where f is the optical frequency, and E_0 the maximum amplitude of electric field. A solution to the differential waveguide equation given in (1) above is

$$H_y = Ae^{ix(n^2k^2-\beta^2)^{1/2}} + Be^{-ix(n^2k^2-\beta^2)^{1/2}} \qquad (3)$$

and therefore E_z given in (2) above can be written as

$$E_z = (-i/n^2\omega E_0)\{Ai(n^2k^2-\beta^2)^{1/2}e^{ix(n^2k^2-\beta^2)^{1/2}} - Bi(n^2k^2-\beta^2)^{1/2}e^{-ix(n^2k^2-\beta^2)^{1/2}}\} \qquad (4)$$

A and B are constants obtained from the solution of the different equation. They will be discussed later.

The four layers in the sensor (cladding, metal, overlay, and sample) each have a different refractive index and therefore produce a different expression for H_y and E_z from eqs 3 and 4 above. These equations for H_y and E_z are shown below

$$H_y^{\text{sample}} = Fe^{-i(n_s^2k^2-\beta^2)^{1/2}x}$$

$$H_y^{\text{overlay}} = Ce^{i(n_o^2k^2-\beta^2)^{1/2}x} + De^{-i(n_o^2k^2-\beta^2)^{1/2}x}$$

$$H_y^{\text{metal}} = Ae^{i(n_m^2k^2-\beta^2)^{1/2}x} + Be^{-i(n_m^2k^2-\beta^2)^{1/2}x}$$

$$H_y^{\text{cladding}} = Ee^{i(n_c^2k^2-\beta^2)^{1/2}x}$$

$$E_z^{\text{sample}} = (-i/n_s^2\omega E_0)(-Fi(n_s^2k^2 - \beta^2)^{1/2}e^{-i(n_s^2k^2-\beta^2)^{1/2}x})$$

$$E_z^{\text{overlay}} = (-i/n_o^2\omega E_0)(Ci(n_o^2k^2 - \beta^2)^{1/2}e^{i(n_o^2k^2-\beta^2)^{1/2}x} - Di(n_o^2k^2 - \beta^2)^{1/2}e^{-i(n_o^2k^2-\beta^2)^{1/2}x})$$

$$E_z^{\text{metal}} = (i/n_m^2\omega E_0)(Ai(n_m^2k^2 - \beta^2)^{1/2}e^{i(n_m^2k^2-\beta^2)^{1/2}x} - Bi(n_m^2k^2 - \beta^2)^{1/2}e^{-i(n_m^2k^2-\beta^2)^{1/2}x})$$

$$E_z^{\text{cladding}} = (-i/n_c^2\omega E_0)(Ei(n_c^2k^2 - \beta^2)^{1/2}e^{i(n_c^2k^2-\beta^2)^{1/2}x}) \qquad (5)$$

where n_s is the sample index, n_o is the overlay index, n_m is the metal index, n_c is the cladding index, n_e is the fiber effective index, $t = d_2 - d_1$ = overlay thickness, λ is the optical wavelength, $k = 2\pi/\lambda$, $\beta = n_e k$, d_1 is the metal thickness, and d_2 is the metal thickness + overlay thickness. The sample and fiber layers contain only one term because the second term would explode as the x-component moved to ± infinity. Waveguide calculations typically ignore this second term to allow solution of the dispersion equation.

Electromagnetics dictates that electric and magnetic fields must be continuous across a charge and current free material boundary. In other words, there can be no discontinuity in the fields across the boundary between two dissimilar materials. Therefore the H_y and E_z fields on each side of a layer boundary must be equal at the boundary. With the following substitutions to simplify the writing of the equations, the H_y and E_z fields are equated across the sample/overlay, overlay/metal, and metal/cladding boundaries.

Let

$$\alpha = (\beta^2 - n_s^2k^2)^{1/2}$$

$$\Delta = (\beta^2 - n_m^2k^2)^{1/2}$$

$$\rho = (\beta^2 - n_c^2k^2)^{1/2}$$

$$\gamma = (\beta^2 - n_o^2k^2)^{1/2}$$

$H_y^{\text{sample/overlay}}$ $(x = d_2)$: $Fe^{-\alpha d_2} = Ce^{\gamma d_2} + De^{-\gamma d_2}$

$H_y^{\text{overlay/metal}}$ $(x = d_1)$: $Ce^{\gamma d_1} + De^{-\gamma d_1} = Ae^{\Delta d_1} + Be^{-\Delta d_1}$

$H_y^{\text{metal/cladding}}$ $(x = 0)$: $A + B = E$

$E_z^{\text{sample/overlay}}$ $(x = d_2)$: $(1/n_s^2)(-F\alpha e^{-\alpha d_2}) = (1/n_o^2)(C\gamma e^{\gamma d_2} - D\gamma e^{-\gamma d_2})$

$E_z^{\text{overlay/metal}}$ $(x = d_1)$: $(1/n_o^2)(C\gamma e^{\gamma d_1} - D\gamma e^{-\gamma d_2}) = (1/n_m^2)(A\delta e^{\Delta d_1} - B\delta e^{-\Delta d_1})$

$E_z^{\text{metal/cladding}}$ $(x = 0)$: $(1/n_m^2)(A\delta - B\delta) = (1/n_c^2)(E\rho)$ (6)

These six equations (6) are in terms of six unknowns, A–F, which are the constants obtained from solving the differential

(19) Marcuse, D. *Theory of Dielectric Optical Waveguides*; Academic Press: New York, 1974.

equation (1). The six equations are algebraically reduced to two equations and two unknowns by simple substitution. The two resulting equations are of the form

$$a_1A + b_1B = 0$$

$$a_2A + b_2B = 0$$

where A and B still represent the constants obtained from solving the differential equation (1), and the a and b terms result from the simple substitution process mentioned above and are given by

$$a_1 = \rho/n_c^2 - \Delta/n_m^2$$

$$b_1 = \Delta/n_m^2 - \rho/n_c^2$$

$$a_2 = [e^{(\gamma+\Delta)d_1}]\{\gamma/n_o^2 - \Delta/n_m^2\} - [e^{(2\gamma d_2 - \gamma d_1 + \Delta d_1)}]\Upsilon\{\gamma/n_0^2 + \Delta/n_m^2\}$$

$$b_2 = [e^{(\gamma-\Delta)d_1}]\{\gamma/n_0^2 + \Delta/n_m^2\} + [e^{(2\gamma d_2 - \gamma d_1 + \Delta d_1)}]\Upsilon\{\Delta/n_m^2 - \gamma/n_o^2\} \quad (7)$$

where

$$\Upsilon = [(\gamma/n_0^2) + (\alpha/n_s^2)]/[(\gamma/n_o^2) - (\alpha/n_s^2)]$$

The dispersion equation is obtained by placing the a and b terms of the two equations into a 2 × 2 matrix.

$$\begin{bmatrix} a_1 & b_1 \\ a_2 & b_2 \end{bmatrix} \qquad a_1b_2 - a_2b_1 = 0$$

The determinant of this matrix must equal zero in order for a solution to the dispersion equation to exist. This solution will indicate the conditions necessary to achieve surface plasmon resonance on the four-layer optical fiber sensor. The determinant is set equal to zero and then rearranged to solve for d_2. The resulting dispersion equation is shown:

$$d_2 = \ln([[\Delta/n_m^2 + \rho/n_c^2][e^{(\gamma+\Delta)d_1}][\gamma/n_o^2 - \Delta/n_m^2] - [\rho/n_c^2 - \Delta/n_m^2][e^{(\gamma-\Delta)d_1}][\gamma/n_o^2 + \Delta/n_m^2]]/[[\rho/n_c^2 - \Delta/n_m^2][e^{-(\gamma+\Delta)d_1}]\Upsilon[\Delta/n_m^2 - \gamma/n_o^2] + [\Delta/n_m^2 + \rho/n_c^2][e^{(\Delta-\gamma)d_1}]\Upsilon[\gamma/n_o^2 + \Delta/n_m^2]])/2\gamma \quad (8)$$

Upon selection of a fiber, laser, metal, and metal thickness, all of the parameters in eq 8 are fixed except for sample refractive index (n_s), overlay refractive index (n_o), and overlay thickness (t). If eq 8 is plotted as overlay thickness (t) as a function of the overlay index (n_o), a family of curves results. Each member of the family represents the conditions necessary to achieve surface plasmon resonance for a different sample refractive index. Each curve will indicate the thickness of the overlay, based on its refractive index, needed to generate SPR for a given sample index. Equation 8 was solved and plotted using Matlab version 3.5 software from The Mathworks.

Figure 4a shows such a plot for an optical wavelength of 780 nm, a 34-nm-thick silver metal film, and Corning Flexcore 850 singlemode fiber, with a core index of 1.4603, a cladding index of 1.4537, and an effective index of 1.457. The results show both a real and an imaginary portion to the overlay thickness for a sample index of 1.350. Since an imaginary thickness is not possible, only that portion of the plot where the imaginary portion is zero is considered as the functioning range of the sensor. Several features of this plot are of interest. First, the curve slopes downward as the overlay index increases. This behavior was expected because less overlay is needed to increase the "effective" index of the plasmon sampling region as the index of that overlay increases. Second, a sharp, semiinfinite peak is seen at an overlay index of 1.419. This index, as will be discussed later, exactly matches the experimentally determined and theoretically predicted sample index needed to generate SPR on this system if no overlay were present. On the basis of these two observations a high degree of confidence is placed on the derived dispersion equation. Figure 4b shows a plot of the dispersion equation for a family of sample refractive indices.

EXPERIMENTAL SECTION

Sensor Fabrication. In order to access the evanescent field surrounding the core of the fiber a short section of the lateral surface of the fiber's cladding is removed by polishing. A 14-in.-long section of the Corning Flexcore fiber had approximately 1 in. of its plastic jacket removed with a blade, and then it was bonded to a curved aluminum polishing substrate as shown in Figure 5. The polishing was carried out on a grinding wheel with 1.0-μm grit polishing paper which was rotated and flushed with water. The curved aluminum polishing substrate (with fiber attached) was lowered onto the polishing wheel and the polishing procedure monitored by measuring throughput of a helium–neon laser beam in the fiber. When the polishing reaches the evanescent field the laser intensity through the fiber begins to decline and the polishing procedure may be terminated.

The fiber was next coated with metal and dielectric layers by vacuum vapor deposition. The fiber, still attached to the polishing substrate, was placed on the target of the vacuum unit and deposition carried out at approximately 5×10^{-6} Torr. The coating thickness may be controlled with a quartz crystal oscillator thickness monitor.

The overlay material chosen for application to the metal should have a high refractive index, so only a thin layer need be deposited. The material should have a low melting point to promote vapor deposition and should be insoluble in the chemical sample to be analyzed. Figure 6 shows a plot of the dispersion equation in the form of thickness of silicon monoxide overlay versus sample refractive index for the Flexcore fiber coated with 34 nm of silver. This plot indicates the thickness of silicon monoxide overlay needed to generate surface plasmon resonance for a given sample refractive index.

Apparatus. After polishing and coating, the fiber was placed into the instrumentation as shown in Figure 7. The fiber was housed in a specially designed plexiglass flow cell which contains two tubing attachments to allow the introduction of chemical samples. The cell had a sample volume of approximately 2 mL and was sealed around the fiber with HPLC fittings. The optical source was an output polarized, 4 mW diode laser operating at 780 nm and the detector a photodiode housed in a specially fitted plastic tube to reduce stray light. The current output of the photodiode was routed through an operational amplifier wired as a current-to-voltage

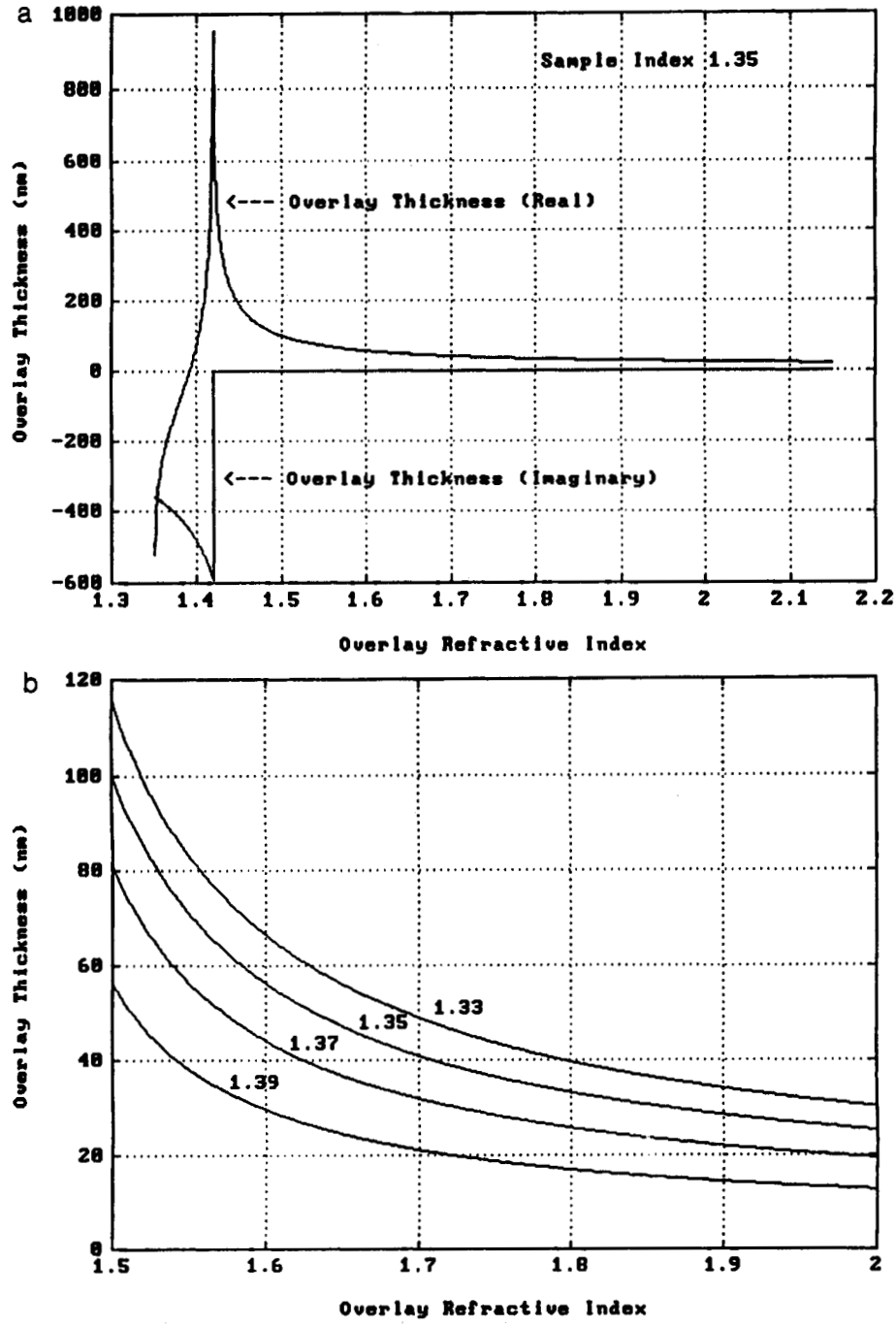

Figure 4. (a) Plot of four-layer sensor dispersion equation. (b) Family of curves of four-layer dispersion equation.

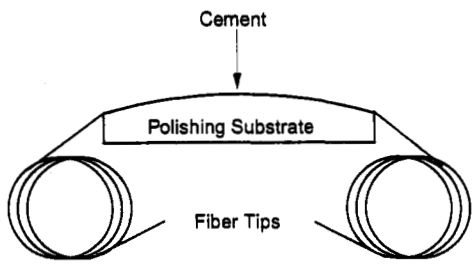

Figure 5. Single-mode optical fiber bonded to polishing substrate.

convertor with variable gain. The output of the amplifier was collected by a handheld data logger as a 0–2000-mV signal. Optical alignment of the laser, fiber, and photodetector is achieved with a three-dimensional translational stage and brass fiber chucks. The laser beam was focused onto the fiber core with a 10× microscope objective which was attached to the laser housing.

The laser beam was launched into the fiber so that the plane of polarization is perpendicular (TM) to the metal film coated on the fiber. Polarization is maintained through the short length of fiber used for sensor construction. If longer sections of fiber (several feet or more) are used, then a polarization preserving or polarizing fiber may be necessary to maintain the integrity of the TM polarization. Round core fibers will scramble polarization with distance.

Reagents. Silver (99.999%) was obtained in 3-mm pellet form from Johnson-Matthew/Aesar, silicon monoxide (99.9%) was obtained from Alfa Chemicals in powdered form, silicon dioxide (99.9%) was obtained from Johnson-Matthew/Aesar

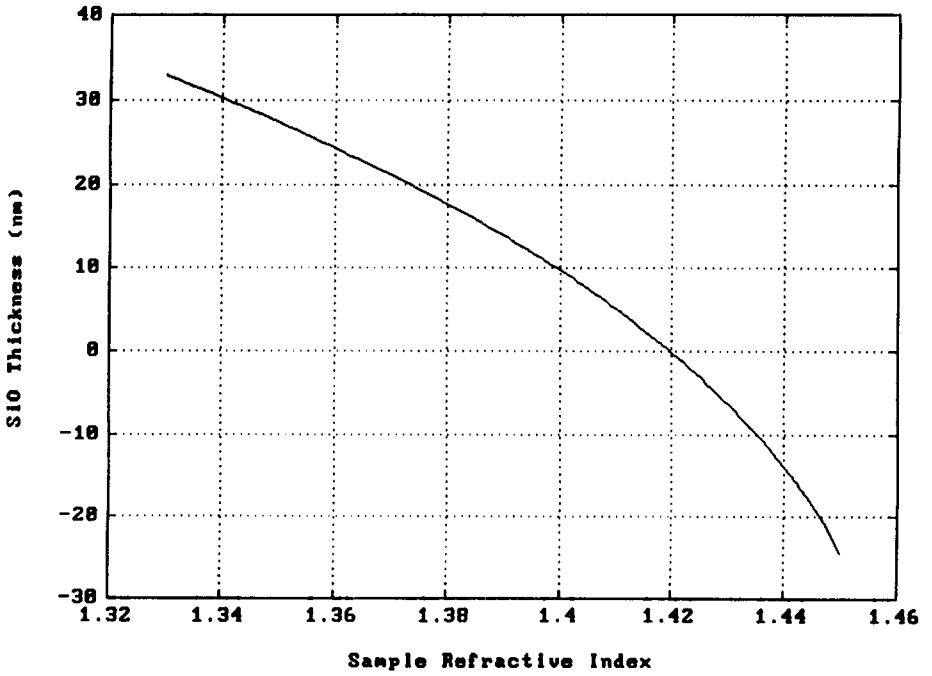

Figure 6. Four-layer dispersion equation plotted as silicon monoxide overlay thickness vs sample refractive index.

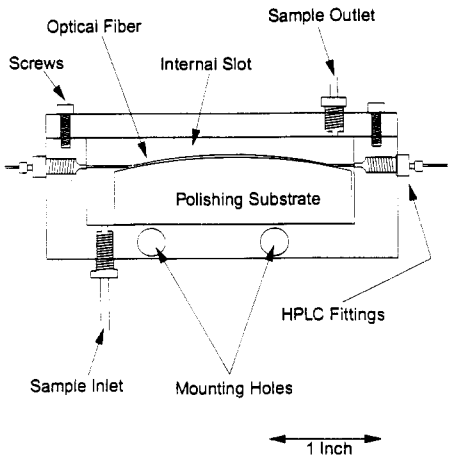

Figure 7. Plexiglass flow cell with single-mode fiber and polishing substrate.

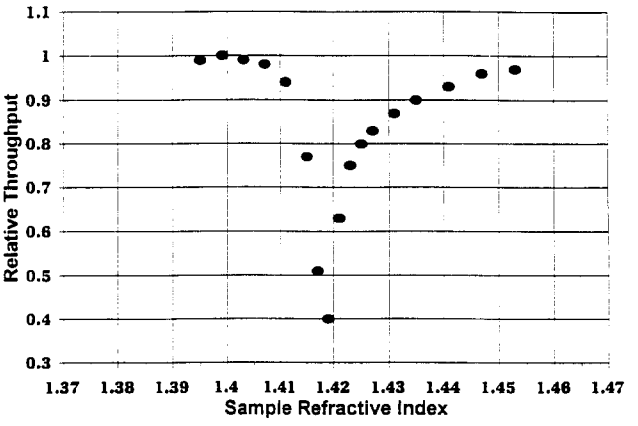

Figure 8. Three-layer SPR data: Cargille refractive index fluids on three-layer sensor.

in powdered form, and sucrose was obtained from Fisher Scientific. Refractive index matching fluid standards (n = 1.400–1.450) were obtained from Cargille Laboratories.

Procedure. One of the polished Corning Flexcore fibers was coated with 34 nm of silver by vacuum deposition but received no overlay material. This fiber was placed into the instrumentation shown in Figure 7 and tested by successive applications of Cargille Laboratories refractive index matching fluids to its sensing area. After application of each fluid the detector signal was recorded, and then the fluid was rinsed from the fiber with hexane to clean the silver surface. The dispersion equations in ref 4 indicate that a sample index of 1.4197 should promote plasmon resonance. Typical data shown in Figure 8 show a minimum at a sample index of 1.419. This refractive index value not only matches the value predicted by ref 4 but also matches the sharp peak in the four-layer dispersion equation plot (Figure 4a) in this work. In this sensor configuration the 1.419 refractive index fluid can be thought of as either a semiinfinitely thick overlay or as a sample layer without an overlay, depending upon whether one uses a three-layer or four-layer dispersion equation.

Silicon monoxide was chosen as an overlay material because it has a relatively high refractive index (1.928 at 780 nm), has a reasonable melting point (~1700 °C) so that it can be easily vapor deposited, and is insoluble in water. Equation 8 was solved for λ = 780 nm, n_o = 1.928, n_m = 5.5i (silver), d_1 = 34 nm (silver thickness), and Corning Flexcore 850 single mode fiber, for a sample index of 1.350. The results indicated that 27.4 nm of SiO would be needed to generate SPR under the given conditions. Vacuum deposition was carried out with the application of 34 nm of silver and 27.4 nm of silicon monoxide. The fiber was then placed in the instrument, and refractive index solutions of sucrose (0–42%) in water were applied sequentially. Typical results are shown in Figure 9. A second silvered fiber was coated with 32.2 nm of silicon monoxide, and a third fiber was coated with 36.8 nm of SiO. The same sucrose solutions were applied to the sensing region of those fibers. The results are listed in Table 1.

Testing of the device with sucrose solutions demonstrates the feasibility of use of the modified fiber as a chemical sensor.

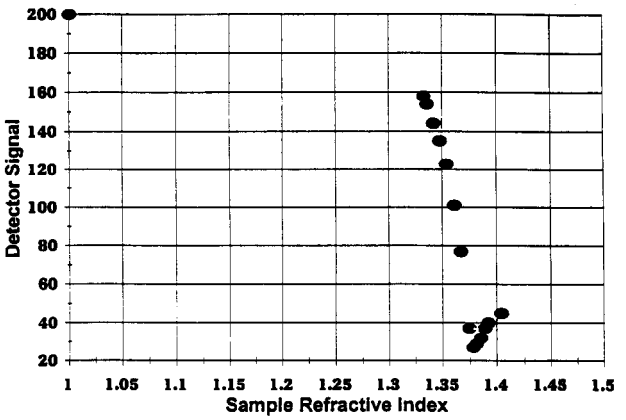

Figure 9. Four-layer SPR data: sucrose solution index fluids on four-layer sensor with silicon monoxide overlay.

Table 1[a]

SiO thickness (nm)	measured resonance index
27.4	1.389
32.2	1.381
36.8	1.344

[a] Sample refractive index generating maximum surface plasmon resonance for several SiO overlay thicknesses.

Sucrose serves as a surrogate analyte. Although surface plasmon resonance on the four layer system is not specific in its own right, since any chemical analyte near the sensor surface will alter the refractive index of the plasmon sampling region. Specificity could be achieved by adding chemically or biologically specific compounds. See, for example, refs 12–14.

Silicon dioxide was also tested as an overlay material. It has a refractive index of 1.54, is easily vacuum deposited, and is insoluble in nonbasic aqueous samples. Equation 8 was solved for $\lambda = 780$ nm, $n_o = 1.54$, $n_m = 5.5i$ (silver), $d_1 = 50$ nm (silver thickness), and Corning Flexcore fiber. A sensor was constructed with 50 nm of silver and 74.5 nm of silicon dioxide using the polishing and deposition procedures listed above. The device was tested with the sequential application of sucrose solutions (0–40%) having refractive indices between 1.333 and 1.40. The results are shown in Figure 10 for two trials. The dispersion equation predicts SPR at a sample index of approximately 1.32.

RESULTS AND DISCUSSION

A dispersion equation has been developed and solved which accurately predicts the operation of an SPR sensor in a four-layer geometry. With the application of a suitable overlay, chemical samples of a wide range of refractive index can be monitored, including aqueous samples. In all cases the application of test refractive fluids showed the surface plasmon resonance condition at a sample index within about 3% of that predicted by the dispersion equation. Differences between the predicted and actual resonance points are most likely a result of inaccuracies in the vapor deposition process and the simplifying assumptions used in solving the dispersion equation. Sensors constructed with silicon monoxide overlays tended to yield resonance at samples slightly higher than predicted (3%).

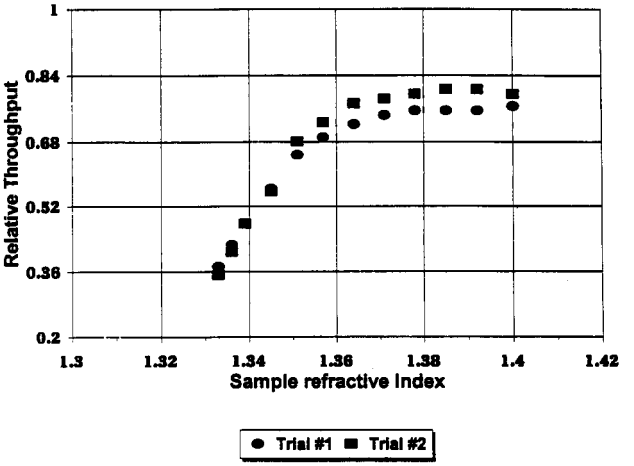

Figure 10. Four-layer SPR data: sucrose solution index fluids on four-layer sensor with silicon dioxide overlay.

This was attributed to oxidation of the surface layer of SiO to SiO_2 by either exposure to atmosphere or aqueous samples. This surface oxidation was confirmed by surface analysis.

The device described here could be used as a chemical or biochemical sensor if it were configured to monitor a reaction whose refractive index passed into or through the sharp minima shown in Figures 8–10. Possible applications of the four-layer sensor system include monitoring biochemical reactions on the surface of the overlay, determination of chemial concentration, as a refractive index detector for liquid chromatography, as a process control microsensor, and as a corrosion monitoring device.

With regard to microscalability, the minimum surface area and plasmon sampling volume of the sensor depend on the diameter of the fiber core, the length of the polished/coated section, and the plasmon sampling depth. The Corning Flexcore fiber has a core diameter of approximately 5 μm and is polished along approximately 2 mm of its length. This gives the sensor an active surface area of approximately 5×10^{-6} m by 2×10^{-3} m, or 10^{-8} m^2 (10^{10} nm^2). If a biomolecule of interest covers approximately 250 nm^2, then only 4×10^7 molecules (7×10^{-17} mol) are required to form a monolayer. If one estimates the molecular weight of the biomolecule at 150 000 then this surface monolayer represents only about 10 p of material. Monolayer coverage has been monitored using the prism-based device, and the sensitivity of the fiber-based device is similar to the prism-based SPR sensors.

If one assumes a plasmon sampling depth of 200 nm above the 10^{-8} m^2 metal surface, then the theoretical minimum sample volume is 2×10^{-9} mL or 2 nL.

Future improvements include the use of polarization-maintaining optical fibers, where the TE polarization could be used as a reference arm, while the TM polarization is used as the signal arm. The two polarizations could be separated by a birefringent optical crystal or a polarization separating fiber-optic coupler. Fiber-optic couplers are devices which separate the light in an optical fiber into two separate fibers. Devices are available commercially which separate the two polarizations in this fashion. By separating the polarizations onto two photodetectors one could ratio the two signals to correct for fluctuations in the laser beam caused by source or temperature drift.

Several potential design considerations will allow for a variety of sampling techniques for the device in order to achieve disposability. The sensing element could be located on a short fiber loop that is connectorized allowing it to be easily attached and removed from a prealigned optical source and photodetector. This type of connector technology is commonplace in the fiber-optic communications industry. The sensing loop could be dipped into the sample of interest. The disposable sensor strand could also be connected to one leg of a fiber-optic coupler which has an optical source and photodetector on other legs. Many variations are possible.

Other improvements could be achieved through investigation of the optimum overlay material and methods of thin film production.

ACKNOWLEDGMENT

The authors thank Mr. Eric Ellis and Dr. Aicha Elshabini-Riad for valuable discussions and assistance with vacuum evaporation of thin films, Dr. Ashish Vengsarkar and Mr. Brian Fogg for assistance with SPR theory, Mr. Fred Blair and Mr. John Miller for assistance with component design and construction, and Mr. Andrew Leoni of Corning Glass and Mr. John McAlarney of Andrew Corporation for supplying optical fibers. This work was partially funded by the Monsanto Chemical Co.

Received for review October 18, 1993. Accepted January 11, 1994.®

® Abstract published in *Advance ACS Abstracts*, February 15, 1994.